

Influence of Disk Dressing Process on Increased Grinding Performance

H. BASERIⁱ, S.M.REZAEIⁱⁱ, A.RAHIMIⁱⁱⁱ, M.REZAEIAN^{iv}

ABSTRACT

A new mathematical model of the dressing of grinding wheels by diamond disk dresser is developed. It predicts the components of dressing forces between the diamond grits of a rotating disk dresser and the grits of an alumina grinding wheel. This model is based on the fracture of grits and the contact forces between dresser and grits. It considers the kinematical influences and, in particular, speed ratio of the dressing process. Dressing forces are measured experimentally and are compared with theoretical calculation. Theoretical results closely match with the experimental findings. The variation of dressing forces versus speed ratio and dressing feed rate are presented at three depth of dressing. At each case, the grinding forces were measured experimentally and the effect of changing dressing parameters on the grinding performance is analyzed.

KEYWORDS

Disk dressing; Dressing forces; Wheel topography; Grinding

1. INTRODUCTION

The final surface topography generated on a grinding wheel is influenced and determined by the dressing conditions. Dressing is a process to remove wheel material mainly by virtue of brittle fracture. The fracture involved in a dressing process includes the fracture of individual grains and the localized fracture of the bond material around the grains. The actual topography arises from the process of grit fracture and/or bond fracture. The wheel topography and the conditions under which it is prepared have a profound influence upon the grinding performance clearly evidenced by the grinding forces, power consumption, cutting zone temperatures, and the surface finish of the workpieces [1]. Improved grinding process control should be obtainable if a more detailed understanding of the dresser-wheel interactions is understood.

Several authors have presented models of the relation between force produced by the interaction of the grinding wheel and the dresser and grinding performance. Torrance and Badger [2] predicted dressing force and number of active grits per unit area against depth and their statistical average slope from the dressing conditions and wheel properties and compared with the measured topography. Takagi and Meng [3] used the dressing force as a measure

to characterize the dressing process. Huang [4] measured the dressing intensity, i.e., the average force per grain, as grinding force, wheel life and surface roughness and examined the effect of the dressing on the grinding performance. Pruzak et al. [5] describe the effects and importance of measured disk dressing factors on grinding performance.

In this paper, a new method of modeling of the dressing forces is described. Then, the effect of changing dressing parameters on the grinding performance is analyzed.

2. PREDICTIVE MODEL OF GRAIN'S FRACTURE FORCE

During the dressing process, grinding wheel surface is generated by fracture of the grain at bond, fracture within the grain. These are referred to, respectively, as bond fracture and grain fracture. Dressing speed ratio q as shown in Figure 1(a) is defined as:

$$q = \frac{V_r}{V_s} \quad (1)$$

V_r is surface speed of the disk dresser and V_s is surface speed of the grinding wheel.

If the diamond dresser infeed into the wheel is a_r , the direction of cutting speed of both dresser and the wheel at the contact point A can be shown as in Figure 1(a).

Now it is considered that the dresser is moving across the wheel. As it can be seen from Figure 1(b), it is

ⁱPh.D. Student of Mechanical Engineering, Amirkabir University of Technology, Tehran, Iran (e-mail: baseri@aut.ac.ir).

ⁱⁱ Associate Professor of Mechanical Engineering, Amirkabir University of Technology, Tehran, Iran (e-mail: smrezaei@aut.ac.ir).

ⁱⁱⁱ Assistant Professor of Mechanical Engineering, Amirkabir University of Technology, Tehran, Iran (e-mail: rahimi@aut.ac.ir).

^{iv} Assistant Professor of Mechanical Engineering, Amirkabir University of Technology, Tehran, Iran (e-mail: rezaeian@aut.ac.ir).

assumed that the dresser tip is tangent to the grit in the first pass of the rotation of the wheel. Due to the dressing cross feed s_d , the dresser tip contacts the grit on the wheel in the second pass (dashed curve in Figure 1(b)) and crushes the grit so that the circular intersection area with radius b is removed. Thus, the compressive fracture forces F_{yf} and F_{nf} act and the stress on the grit reaches the maximum fracture stress for the grit.

In brittle materials, the fracture stress is dependent on the strain rate [6]. If σ_0 is the stress of grit at strain rate $\dot{\epsilon} = 1$, then the fracture stress σ_f at the other strain rates for alumina grit is as follow [7]:

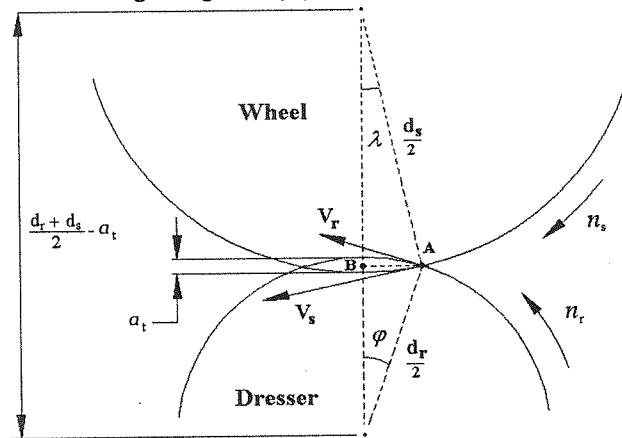
$$\sigma_f = \sigma_0(1 + 0.0078 \ln \dot{\epsilon}) \quad (2)$$

$\dot{\epsilon}$ is given by:

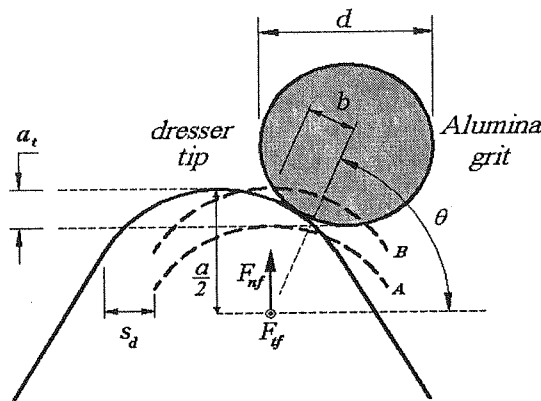
$$\dot{\epsilon} = \frac{\delta_{\max} / d}{t} \quad (3)$$

δ_{\max} is maximum deflection at maximum fracture force F_R for alumina grit, d is average diameter of alumina grit and t is the duration of impact.

For calculating the strain rate $\dot{\epsilon}$, it can be considered that the duration of impact between the dresser edge and the alumina grit is given by [8]:



(a)



(b)

Figure 1: Geometry of disk dressing; (a) Front view of dresser and wheel; (b) Lateral contact of disk dresser tip and the grit at points A and B

$$t = 2.94 \frac{\delta_{\max}}{\Delta V} \quad (4)$$

ΔV is the relative speed. Therefore:

$$\dot{\epsilon} = \frac{\Delta V}{2.94d} \quad (5)$$

Using stress formula around a load point, this will give a fracture force F_R on a grit as follows [8]:

$$F_R = \sqrt{F_{yf}^2 + F_{nf}^2} = \frac{2\pi b^2}{(1 - 2\nu_g)} \sigma_f \quad (6)$$

σ_f is fracture stress for the alumina grit, ν_g is poisson's ratio of alumina grit and b is radius of circular fracture area in Figure 1(b) and is given by:

$$b = \sqrt{\frac{a^2}{4} - \left(\frac{a^2 + 4L^2 - d^2}{8L}\right)^2} \quad (7)$$

a is the diameter of the dresser tip, d is the mean diameter of the grit and L can be stated as:

$$L = \frac{0.5(a + d) - a_t}{\sin \theta} \quad (8)$$

θ is:

$$\theta = \tan^{-1} \left(\frac{0.5(a + d) - a_t}{\sqrt{a_t(a + d) - a_t^2 - s_d}} \right) \quad (9)$$

s_d is the cross feed of dressing in mm/rev and is given by:

$$s_d = \frac{\pi d_s v_d}{V_s} \quad (10)$$

where v_d is cross feed of the dresser in mm/min.

It is assumed that direction of the fracture force F_R is the same as the direction of relative velocity $\Delta \vec{V}$, which is equal to $\vec{V}_r - \vec{V}_s$. Therefore referring to Figure 2, $\Delta \vec{V}$ is:

$$\Delta \vec{V} = (-V_r \cos \phi + V_s \cos \lambda) \hat{i} + (V_r \sin \phi + V_s \sin \lambda) \hat{j} \quad (11)$$

and,

$$\Delta V = V_s \sqrt{1 + q^2 - 2q \cos(\phi + \lambda)} \quad (12)$$

λ is the wheel contact angle and ϕ is the dresser contact angle. Referring to Figure 1(a), these angles can be calculated as follows:

$$\sin \lambda = \frac{d_r \sqrt{1 - A^2}}{d_r + d_s - 2a_t} \quad (13)$$

$$\sin \phi = \frac{d_s}{d_r} \sin \lambda \quad (14)$$

where,

$$A = 2\{[(d_s + d_r)/2 - a_t]^2 - (d_s/2)^2 - (d_r/2)^2\} / (d_r d_s) \quad (15)$$

d_s is wheel diameter, d_r is dresser diameter and a_t is depth of dressing. Referring to Figure 2, angle θ_1 is given by:

$$\theta_1 = \cos^{-1} \left(\frac{-q \cos \varphi + \cos \lambda}{\sqrt{1 + q^2 - 2q \cos(\varphi + \lambda)}} \right) \quad (16)$$

Therefore, fracture force components on grits can be considered as follows:

$$F_{tf} = \sum_1^{N_g} F_{tf,i} = \sum_1^{N+1} F_{R,i} \cos \theta_{1,i} \quad (17)$$

$$F_{nf} = \sum_1^{N_g} F_{nf,i} = \sum_1^{N+1} F_{R,i} \sin \theta_{1,i} \quad (18)$$

N_g is total number of grains, which contacts the dresser tip on arc AB as shown in Figure 1(a). N is integer fraction of N_g , $F_{tf,i}$ and $F_{nf,i}$ are tangential and normal fracture forces on grit i th (within arc AB) and $F_{R,i}$ and $\theta_{1,i}$ as shown as in Figure 3 are given by:

$$F_{R,i} = \frac{2\pi \sigma_{f,i}}{1 - 2\nu_g} \cdot \left(\frac{N_g - N + i - 1}{N_g} b \right)^2 \quad (19)$$

$$\theta_{1,i} = \cos^{-1} \left(\frac{-V_r \cos(k_i \cdot \varphi) + V_s \cos(k_i \cdot \lambda)}{\Delta V_i} \right) \quad (20)$$

Where

$$\sigma_{f,i} = \sigma_0 \cdot \left(1 + 0.0078 \ln \frac{\Delta V_i}{2.94d} \right) \quad (21)$$

$$\Delta V_i = V_s \sqrt{1 + q^2 - 2q \cos(k_i(\varphi + \lambda))} \quad (22)$$

$$k_i = \frac{N_g - i + 1}{N_g} \quad (23)$$

To calculate N_g and N , it is assumed that during the dressing process, the removal of the wheel occurs due to the engagement and the collision of the dresser with the grits and the bonding matrix. Referring back to Figure 1(a) which shows the disk dressing process, length of contact is given by:

$$l_g = \overline{AB} = \frac{d_s \sin \lambda}{2} \quad (24)$$

Moreover, area A_g between the grits and the dresser is as follows:

$$A_g = l_g b_d \quad (25)$$

b_d is the dressing tool width and referring to Figure 4, is given by:

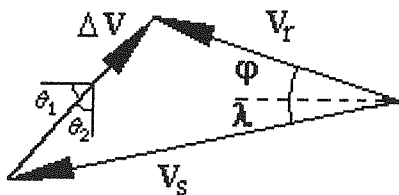


Figure 2. Relative velocity of contact

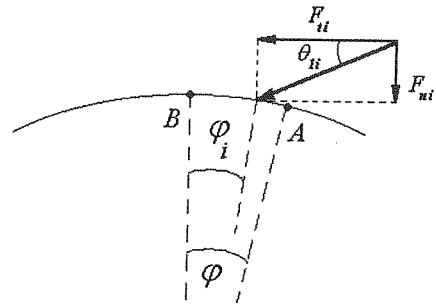


Figure 3. Tangential and normal dressing forces on a grit in angle φ_i

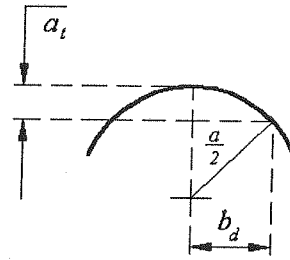


Figure 4. Geometry of disk dresser tip and dressing tool width.

$$b_d = \sqrt{a \cdot a_t - a_t^2} \quad (26)$$

Thus within each dressing stroke the total number of grits N_g is given by:

$$N_g = A_g N_s \quad (27)$$

N_s is number of grains per unit area within the wheel [9]:

$$N_s = \frac{6V_g}{\pi d^2} \quad (28)$$

d is the average grit diameter and V_g is the volume fraction of grits in the wheel and is given by:

$$V_g = 2(32 - S) \% \quad (29)$$

where S is the structure number of the wheel.

Therefore, the number of grains in contact to the dresser is:

$$N_g = 0.5 N_s d_s \sin \lambda b_d \quad (30)$$

3. DETERMINATION OF THE TOTAL DRESSING FORCE COMPONENTS IN THE DRESSING ZONE

The total dressing force has a tangential component F_t , and a normal component F_n . During the dressing process, there will be variation from the nominal value of the depth of dressing set on the machine. It is due to the deflection of the wheel, the individual grit and the dresser. Therefore, a fraction of the total dressing force is used to absorb the deflection of the wheel and so forces F_t and F_n have two parts. First is the total fracture force due to the grain fracture. Second is the contact force due to the elastic wheel deflection. Therefore, it can be written:

$$F_t = F_{tf} - \mu F_{nc} \quad (31)$$

$$F_n = F_{nf} + F_{nc} \quad (32)$$

where F_{tf} and F_{nf} are the total tangential and normal acted force and are given theoretically. F_{nc} is the normal contact force and μ is the coefficient of friction and are achieved experimentally.

A. Determination of the normal contact force (F_{nc}) and coefficient of friction (μ)

As mentioned above, a fraction of the total dressing force used to absorb the deflection of the wheel. Most of the elastic deformation of the wheel is due to the grits and deflection of a grain δ in the surface of a wheel can be assumed to follow an equation as [10]:

$$\delta = B \cdot F_{nc}^n \quad (33)$$

where B is constant, F_{nc} is the normal contact force and n is between 0.4 to 0.7 for various grain size and hardness of the wheels. Also Saini [11] has determined a single grit deflection and found that the grit deflection was a significant percentage of the actual grit depth of cut. Therefore, for depth of dressing a_i can be written:

$$\delta = B_1 \cdot a_i \quad (34)$$

where B_1 is constant. By combining the two last equations, the following can be deduced:

$$F_{nc} = B_2 \cdot a_i^{1/n} \quad (35)$$

B_2 is another constant.

An experiment was conducted to determine constants B_2 and n . For normal contact force to be measured the dresser was fed into the wheel and depth of dressing is a_i . After a few revolutions of the grinding wheel and grain fracture, the normal contact force due to wheel deflection was measured. Increasing the depth of dressing would result in an increase in the normal contact force, as shown in Figure 5. Therefore, the normal contact force can be given by:

$$F_{nc} = 1526 a_i^{1.496} \quad (36)$$

where a_i is in *mm* and F_{nc} is in *Newtons*. It can be evident that parameter n is 1/1.496 which is equal to 0.668. Also, constant B_2 is 1526.

After the measurement of normal contact force, the dresser was kept stationary while the wheel was rotated slowly. Then, the tangential contact force was measured as shown in Figure 6. In this case, the friction factor μ is approximated as 0.42. Normal components of grain's fracture force (F_{nf}) and contact force (F_{nc}) are shown in Figure 7.

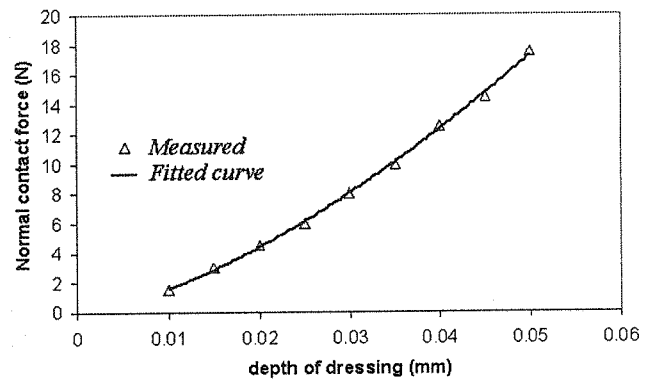


Figure 5. Relation between Normal contact force and depth of dressing for determination the constants B_2 and n (equation 35).

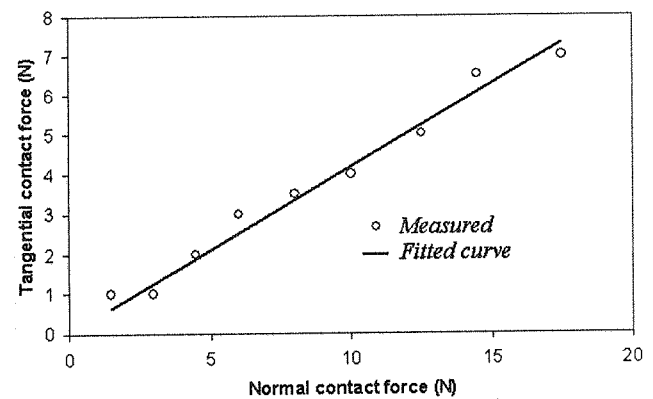


Figure 6: Relation between normal contact force and tangential contact force

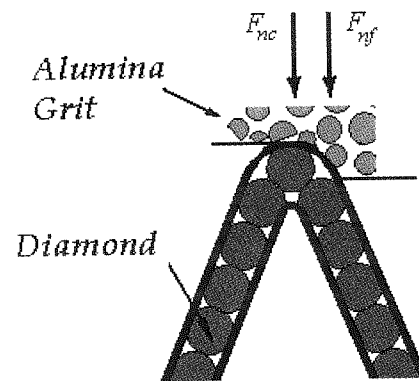


Figure 7: Normal contact force (F_{nc}) and normal fracture force (F_{nf}) on grinding wheel during the dressing process.

4. EXPERIMENTAL SETUP

A. Dressing system

The dressing system setup is illustrated in Figure 8 and Figure 9. It consists of a dressing disk rotated with an electric motor with speed control. The device is placed on the table of the grinding machine with feed control. The axis of the dresser spindle is parallel to the grinding wheel spindle axis. During dressing, the disk is traversed across the wheel width at a constant feed rate. Specifications of the dresser and the grinding wheel are given in Table 1.

For each set of experimental conditions, the dressing operations were repeated three times. The average value is used to minimize experimental errors. The dressing forces were measured by a dynamometer (Kistler 9255 B) and then downloaded into a data acquisition system. The details of the experimental setup are shown in Table 1.

Three parameters namely speed ratio, cross-feed rate and depth of dressing were varied to verify the theoretical analysis. Eight speed ratios, as listed in Table 1, were selected. At each speed ratio, four experiments with different cross-feed rate were conducted. At each set of speed ratio and cross-feed rate, different depths of dressing, were investigated. A total of 84 dressing experiments were carried out.

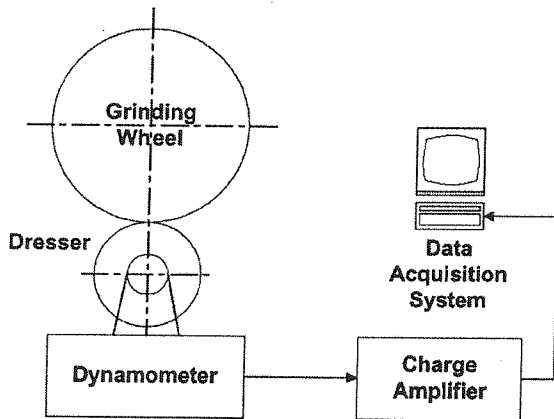


Figure 8. Schematic diagram of the dressing system.

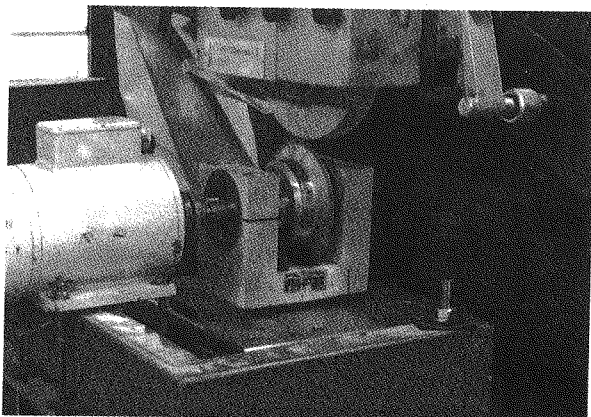


Figure 9. Disk dressing installation.

B. Grinding system

To examine the effect of the dressing conditions on grinding performance, grinding experiments were conducted using a precision surface grinder (Hauni-Blohm HFS204). The dressing-grinding system is illustrated in Figure 10. The vitrified aluminum oxide grinding wheel was dressed using the diamond disk dresser. The grinding conditions are as listed in Table 1. Grinding forces were measured by a dynamometer (Kistler 9255 B) at tangential and normal direction of the wheel.

The workpiece material was SPK 1.2080 with hardness 56 Rockwell C. Workpiece specimens were 100 mm long, 40 mm wide and 7 mm high.

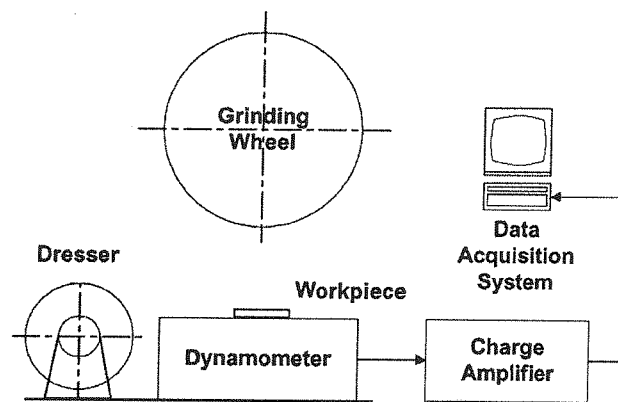


Figure 10. Schematic diagram of the grinding system.

TABLE 1

SUMMARY OF SETUP PARAMETERS FOR DRESSING AND GRINDING

Machine	
Model	Hauni-Blohm HFS204
Spindle speed	1720 rpm
Spindle power	10 kW
Grinding system	
Wheel speed (V_s)	18 m/sec
Bond	Vitreous
Type	A46K6V
Size	200 mm diameter, 20 mm width
Type of abrasive	Aluminum oxide
Grinding depth of cut	0.03 mm
Table speed	3 m/min
Dressing system	
Dresser	Winter
Dimension	130 mm diameter 0.5 mm tip radius
Dressing ratio (q)	0.3, 0.5, 0.6, 0.7, 0.8, 0.85, 0.9, 0.95
Cross-feed rate (v_d)	48, 96, 144, 192 mm/min
Depth of dressing (a_t)	0.03, 0.04, 0.05 mm
Motor	220 V, 14 amps
Max speed	11000 rpm, both direction
Cross-feed driver	Stepper motor 5kg/cm

5. RESULTS, DISCUSSION AND COMPARISON BETWEEN PREDICTED AND EXPERIMENTAL RESULTS

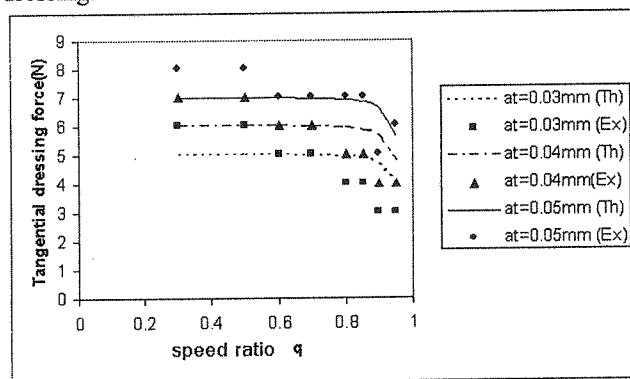
Figures 11 and 12 show the comparison of the theoretical and experimental results. The experiments were repeated for three different depth of dressing. It can be clearly seen that the normal dressing force of the proposed model closely match with those experimentally obtained. But, the agreement for tangential dressing force is not so close.

There are two possible reasons for the deviation between the theoretical and measured tangential dressing force. Firstly, the dressing model assumes that only single

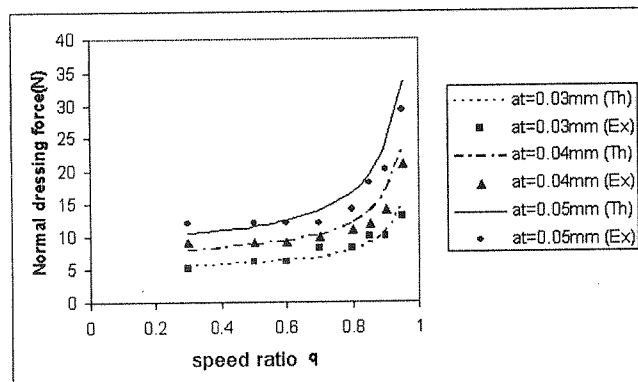
grits are broken from the surface, whereas there is always the possibility that two or more grits might be broken out. Secondly, the dressing model assumes that only the grit fracture occurred and bond fracture did not occur, whereas there is the probability that bond fractures might be occurred. The effects of various parameters are discussed as follows.

A. Effect of speed ratio on tangential dressing force

Figure 11(a) shows the variation of tangential dressing force against speed ratio for various dressing depths. The tangential dressing force decreases with increasing speed ratio. This behavior is independent of dressing depths. In fact, this tendency is constant for various depths of dressing.



(a)



(b)

Figure 11: Predicted (Th) and measured (Ex) forces of dressing versus speed ratio.

It can be argued that with increasing speed ratio, the tangential component of the relative speed ΔV becomes smaller. Due to this effect and referring to Figure 4 the angle $\theta_{1,i}$ is increased. As a result, the tangential dressing force follows a decreasing trend. In low speed ratio, collisions takes place at the tangential direction to alumina grits and shearing forces act on the wheel grits. Then, high attritious wear and small crushing is produced on the grits.

B. Effect of speed ratio on normal dressing force

Figure 11(b) shows the variation of normal dressing force versus speed ratio for three dressing depths. Unlike

the previous case, the normal dressing force increases with increasing speed ratio. This trend has a slow pattern up to the speed ratio +0.8. But the dressing forces suddenly start to rise above this speed ratio. The same argument as for the tangential force can also be applied here.

With increasing speed ratio, the normal component of relative speed ΔV becomes larger. This causes a rise in normal dressing force. In high speed ratio, the collision between dresser tip and the alumina grits takes place at the radial direction of grits. Then, compressive forces act on grits and low attritious wear and large crushing are produced on grits. When speed ratio is 1, full crushing takes place which causes grain cutting edge to become dull. This argument is also in line with the finding of previous researchers conducted by a diamond roll dresser [11].

C. Effect of dressing cross feed rate on dressing forces

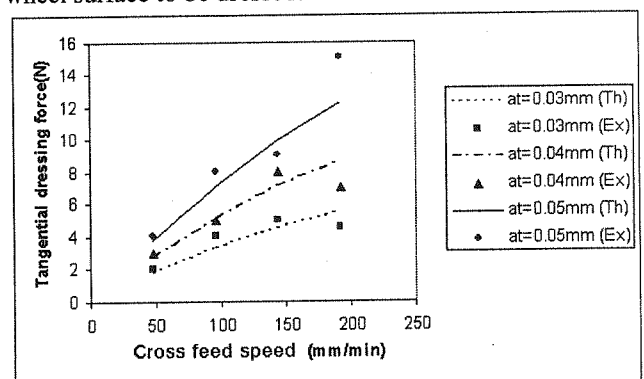
Figure 12(a,b) shows the variation of dressing forces against cross feed for various dressing depths of cut. The dressing forces rise with an increase in dresser cross feed. This increase is independent of dressing depths. With an increase in the dresser cross feed, the fractured sectional force of the grits become larger. It leads to an increase in the fracture force F_R .

D. Effect of speed ratio on grinding forces

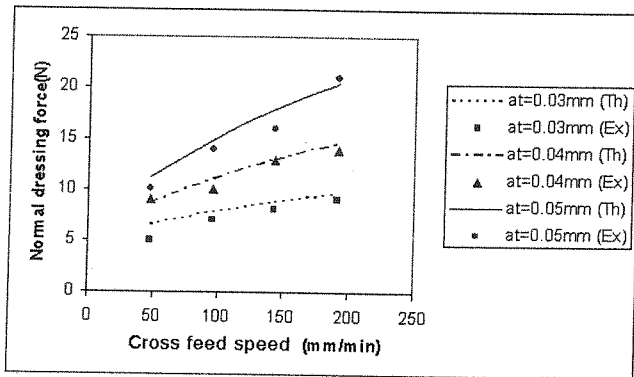
The tangential and normal grinding forces versus speed ratio are shown in Figure 13(a). The grinding forces decrease with increasing speed ratio. As can be seen above, speed ratio +0.8, sharpness of grinding wheel becomes sufficient and the rate of decrease the grinding forces is low. It can, therefore, be argued that speed ratio of +0.8 is optimum. Above this speed ratio, the normal dressing force suddenly rises. This can be determinate the dresser.

E. Effect of dressing cross feed rate on grinding forces

As can be seen in Figure 13(b), tangential and normal grinding forces drop with an increase in dresser cross feed. This means that with faster dresser cross feed rate, sharper grinding wheel can be obtained. If the dresser cross feed is too high, the diamond tool misses some portion of the wheel surface to be dressed.

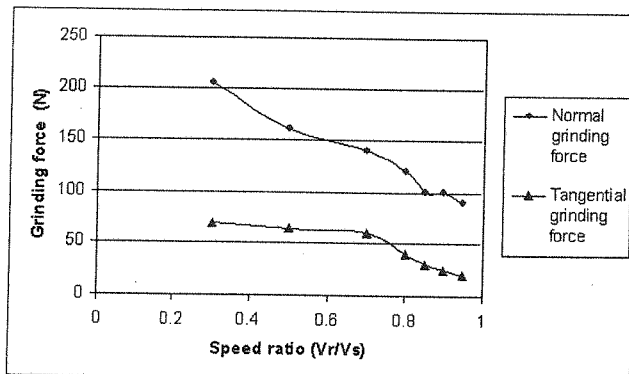


(a)

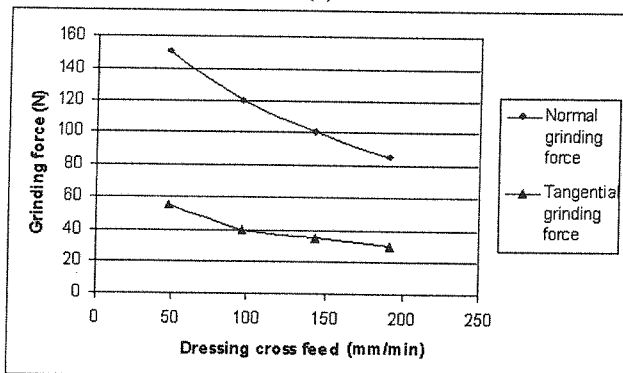


(b)

Figure 12: Predicted (Th) and measured (Ex) forces of dressing versus cross feed rate.



(a)



(b)

Figure 13: (a) measured grinding forces versus speed ratio; (b) measured grinding forces versus dressing cross feed rate.

As a result an inconsistency on the wheel surface is produced. To achieve the smooth and consistent wheel surface, the cross feed should be calculated so that all parts of the wheel surface is dressed.

6. CONCLUSIONS

A new model for the prediction of dressing forces has been developed. It is based on the interaction of the grits of the grinding wheel with the disk dresser. The theoretical results show a good comparison with those obtained experimentally. The model closely demonstrates the relation of the dressing forces against speed ratio, cross feed rate and depth of dressing.

Above speed ratio of +0.8, the normal dressing force suddenly starts to rise. This is also in line with the experimental finding of previous researchers conducted by a diamond roll dresser. Also, the grinding force decreases when speed ratio and dresser cross feed rate are increased.

7. NOMENCLATURE

a	dresser tip diameter
a_t	dressing depth
A	constant
A_g	contact area between dresser and wheel
b	radius of the grit circular fracture area
b_d	dressing tool width
d	mean diameter of the wheel grains
d_r	dresser diameter
d_s	wheel diameter
F_g	resultant fracture force on grit
F_n	normal dressing force
F_t	tangential dressing force
F_{nc}	normal contact dressing force
F_{nf}	normal fracture dressing force
F_{tf}	tangential fracture dressing force
k	counter of the grits in contact angle
l_g	contact length between dresser and wheel
N	integer number of contact grains
N_g	number of contact grains
N_s	number of grains per unit area of the wheel
q	dressing speed ratio
s_d	cross-feed per revolution
S	structure number of the wheel
V_d	cross-feed speed
V_r	surface speed of the dresser
V_s	surface speed of the wheel
ΔV	relative speed between dresser and the wheel
V_g	fraction of grits in the wheel volume
φ	contact angle of the dresser
θ_l	angle between relative speed and horizontal axis
λ	contact angle of the wheel
μ	coefficient of friction between dresser and wheel
ν_g	Poisson's ratio of the grain
σ_f	mean fracture stress of the grain

8. ACKNOWLEDGEMENT

Authors wish to thank *Dr. Amir Abdullah* for his valuable help in the experimental program. The assistance given by the staff of the Machining Research Laboratory of Mechanical Engineering Department of Amirkabir University of Technology is also acknowledged.

9. REFERENCES

- [1] S. Malkin, N.H. Cook, "The wear of grinding wheels. Part 1. Attritious wear, Trans", Trans ASME, Journal of Engineering for Industry 93 (1971) 1120-1128.
- [2] J.A. Badger, A.A. Torrance, "A comparison of two models to predict grinding forces from wheel surface topology", International Journal of Machine Tools & Manufacture 40 (2000) 1099-1120.

- [3] J. Takagi, L. Meng, "Fracture characteristics of grain cutting edge of CBN wheel in truing operation", *Journal of Materials Processing Technology* 62 (1996) 397-402.
- [4] H. Huang, "Effect of truing/dressing intensity on truing /dressing efficiency and grinding performance of vitrified diamond wheels", *Journal of Materials Processing Technology* 117 (2001) 9-14.
- [5] Z. Pruzak, J. A. Webster, I. D. Marinescu, "Influence of dressing parameters on grinding performance of CBN/Seeded Gel hybrid wheels in cylindrical grinding", *International Journal of production Research* 35(1997) 2899- 2915.
- [6] G.R. Johnson, T.J. Holmquist, "A computational constitutive model for brittle materials" in: M.A. Meyers, L.E. Murr, K.P. Staudhammer (Eds.), "Shock-wave and High-strain rate Phenomena in Materials", Marcel Dekker Inc., New York, 1992, p 1075-1081.
- [7] J. Lankford, "Compressive strength and microplasticity in poly crystalline alumina", *Journal of Materials Science* 12 (1977) 791-796.
- [8] S.P. Timoshenko, J.N. Goodier, "Theory of Elasticity", McGraw-Hill, New York, 1970. pp 409-414.
- [9] S. Malkin, *Grinding technology, theory and Applications of Machining with Abrasives*, Ellis Horwood, Chichester, 1989.
- [10] D.P. Saini, R.H. Brown, "Elastic deflection in grinding", *Annal CIRP* 29(1) (1980), 189.
- [11] C. Andrew, T.D. Howes, T. R. Pearce, *Creep feed grinding*, Holt Rinehart and Winston, 1985.

